Research Square

Preprints are preliminary reports that have not undergone peer review.
They should not be considered conclusive, used to inform clinical practice,
or referenced by the media as validated information.

Characterization of Caprock Integrity in CCS Development Based on Shale Core Rock Elasticity of Well SA-001 in the Salaq Basin, Indonesia

Aris Buntoro

arisbuntoro@upnyk.ac.id

Universitas Pembangunan Nasional Veteran Yogyakarta

Allen Haryanto Lukmana

Universitas Pembangunan Nasional Veteran Yogyakarta

Teddy Eka Putra

PT. Pertamina

Dwandari Ralanarko

PT. Pertamina

Research Article

Keywords: Caprock integrity, CCS, rock elasticity, rock mechanics, Mohr–Coulomb failure, Salaq Basin

Posted Date: May 28th, 2026

DOI: https://doi.org/10.21203/rs.3.rs-8893502/v1

License: This work is licensed under a Creative Commons Attribution 4.0 International License.
Read Full License

Additional Declarations: No competing interests reported.

Characterization of Caprock Integrity in CCS Development Based on Shale Core Rock Elasticity of Well SA-001 in the Salaq Basin, Indonesia

Aris Buntoro, Petroleum Engineer & Geoscientist, Petroleum Engineering Department, UPN "Veteran" Yogyakarta, Indonesia
Allen Haryanto Lukmana, Geomechanics Specialist, Petroleum Engineering Department, UPN "Veteran" Yogyakarta, Indonesia
Teddy Eka Putra, Senior Specialist Innovation Geology, Upstream Innovation, PT. Pertamina Hulu Energi, Indonesia
Dwandari Ralanarko, Subsurface Geoscience Lead, Project Carbon Management, PHE Upstream Business Development, Indonesia

*Corresponding author, E-mail: arisbuntoro@upnyk.ac.id

ABSTRACT

The integrity of caprock is a critical factor controlling the long-term safety of Carbon Capture and Storage (CCS) projects. This study presents a comprehensive geomechanical characterization of shale caprock based on laboratory rock mechanics and elastic property measurements from shale core samples of Well SA-001 in the Salaq Basin, Indonesia. Fifteen core plugs from depths between 3546 and 3744 ft MD were subjected to uniaxial and triaxial compressive strength tests, static elastic modulus measurements, and Mohr–Coulomb failure envelope analysis following ASTM D7012 standards. The results indicate ultimate compressive strengths ranging from 10.23 to 112.46 MPa under confining pressures of 0–9.32 MPa. Static Young's modulus varies between 749 and 12,097 MPa, with Poisson's ratios of 0.12–0.20. Mohr envelope analysis reveals cohesion values of 2.23–16.56 MPa and internal friction angles between 33.16° and 45.52°. These mechanical and elastic characteristics indicate that the shale interval possesses moderate to high stiffness and shear strength, supporting its effectiveness as a sealing formation for CCS operations. The integration of elastic properties and failure criteria provides a robust basis for assessing caprock integrity under CO_2 injection-induced stress changes.

Keywords: Caprock integrity, CCS, rock elasticity, rock mechanics, Mohr–Coulomb failure, Salaq Basin

1. INTRODUCTION

Carbon Capture and Storage (CCS) has emerged as a key technology for mitigating anthropogenic CO_2 emissions. A fundamental requirement for safe CCS implementation is the mechanical integrity of the caprock, which must effectively prevent upward migration of injected CO_2 over geological timescales. Mechanical failure, reactivation of pre-existing fractures, or injection-induced tensile or shear failure can compromise storage security.
Shale formations commonly act as caprocks due to their low permeability, fine grain size, and favorable geomechanical properties. However, the response of shale to stress perturbations caused by CO_2 injection depends strongly on its elastic moduli, strength parameters, and failure envelope. Laboratory-derived elastic and strength parameters are therefore essential inputs for geomechanical modeling and injection risk assessment.

This study aims to characterize the integrity of shale caprock in the Salaq Basin using detailed laboratory rock mechanics data from Well SA-001. Emphasis is placed on elastic properties,

compressive strength behavior under varying confining pressures, and Mohr–Coulomb failure parameters relevant to CCS operations.

2. STUDY AREA & GEOLOGY

The Salaq Basin is a sedimentary basin located in the offshore region of Southeast Sumatra, Indonesia. It forms part of the larger Sunda Basin represents a mature and prolific hydrocarbon province, formed by Cenozoic extensional tectonics that generated a series of half-graben depocenters filled with thick syn-rift and post-rift sedimentary successions (Hall, 2002; Martodjojo, 2003; Doust & Noble, 2008). These successions host proven source rocks, high-quality clastic reservoirs, and regionally extensive seals, making the basin not only prolific for oil and gas but also highly prospective for large-scale geological CO_2 storage in future CCS developments (Bradshaw et al., 2007; Doust, 2016).

The Salaq Basin is a north–south–oriented half-graben basin formed by Cenozoic extensional tectonics (Zhu et al., 2018), and was formed during the Eocene (**Figure 1**). This normal fault plays an important role in the deposition and stratigraphic evolution in this region, where the downward movement of the fault block allows the formation of space for sediment deposition (Ralanarko et al., 1998).

The basin is characterized by a complex geological framework dominated by Tertiary sedimentary successions, comprising marine shales, clastic sandstones, and locally developed carbonate deposits (Siregar et al., 1994). These formations play a crucial role in defining the reservoir-caprock system essential for CCS implementation.

Well SA-001 is located in the western part of the Salaq Basin and penetrated a thick shale sequence interpreted as a regional sealing unit, where thick shale deposits serve as potential cap rock for CO_2 storage. These shales are primarily of Miocene age and have been identified as regionally extensive sealing formations overlying sandstone reservoirs (Doust & Noble, 2008). The ability of these formations to function as effective seals is strongly controlled by their elastic behavior, brittleness index, and resistance to fracture initiation and propagation, all of which are essential for assessing the long-term security of geological CO_2 storage (Zoback, 2010).

Core samples analyzed in this study were collected from depths between 3546 and 3744 ft MD, corresponding to the shale interval immediately overlying the target reservoir. These depths represent in-situ stress conditions relevant to future CO_2 injection scenarios.

Geologically, the Salaq Basin has undergone multiple tectonic events, including rifting and subsidence, which have influenced its structural evolution. The presence of extensional faulting in the basin introduces potential risks for CO_2 migration if caprock integrity is compromised (Hall & Morley, 2004). Therefore, a detailed geomechanical assessment integrating shale core analysis from Well SA-001 is necessary to evaluate the sealing efficiency of the caprock and ensure secure CCS development.

This study contributes to a better understanding of the caprock characteristics in the Salaq Basin, providing critical data for future CCS projects in offshore Indonesia. By assessing the rock elasticity and geomechanical behavior of the shale formations, the research aims to

support sustainable carbon storage solutions and minimize the risks associated with CO_2 leakage.

The stratigraphy of the Salaq Basin consists of siliciclastic and carbonate sediments of Eocene to Pleistocene age. Cretaceous crystalline rocks act as the basement that underlies the basin. Overlying is the Banuwati Formation, composed of alluvial fan, fluvial, and lacustrine deposits, marking the beginning of basin filling. Throughout the Oligocene to Miocene, transitional to shallow marine deposits consisting of sandstone, mudstone, coal, and limestone were deposited. The Talang Akar Formation is divided into the Zelda Member and the Gita Member. According to Zhu et al. (2018), the Lower Zelda Member is composed of fluvial sandstone, mudstone, and shale units from subaquatic fans, deltaic fans, deltas, and lacustrine environments. The Upper Zelda Member is composed of deltaic fans, deltas, subaquatic fans, and turbidite fans composed of alternating sandstones, shales, and siltstones, with the main unit consisting of braided river channels containing thick and stacked reservoir sandstones. The Gita Member is dominated by sandstone, organic claystone, and coal. The Baturaja and Gumai Formations represent the final phase of rifting and are regional in nature, characterized by shallow marine deposits of limestone and other fine-grained rocks. The Talang Akar and Baturaja Formations serve as the target reservoirs for carbonaceous sedimentation, while the Gumai Formation serves as the primary cap rock. The general stratigraphy of the Salaq Basin is shown in **Figure 2**.

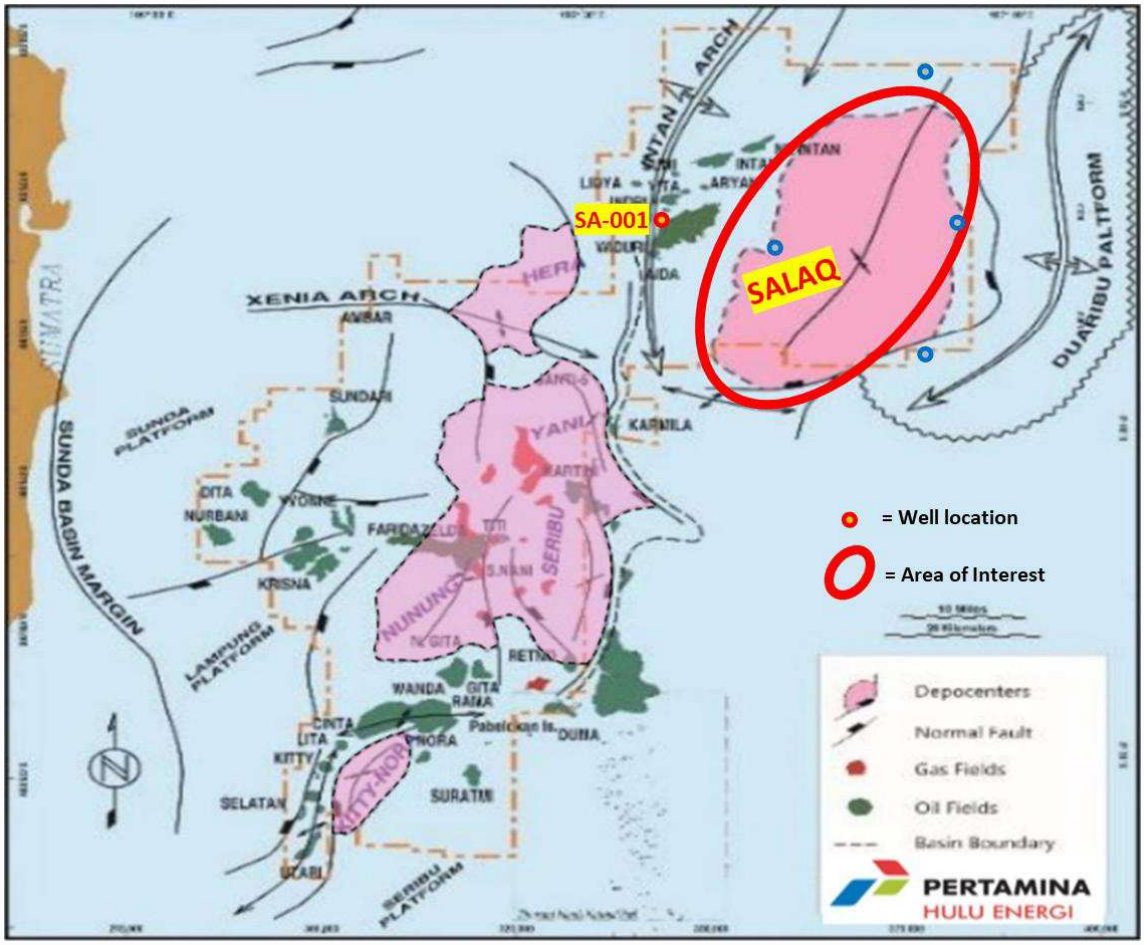


Figure 1. Regional tectonics of the Salaq Basin (Ralanarko et al, 2020)

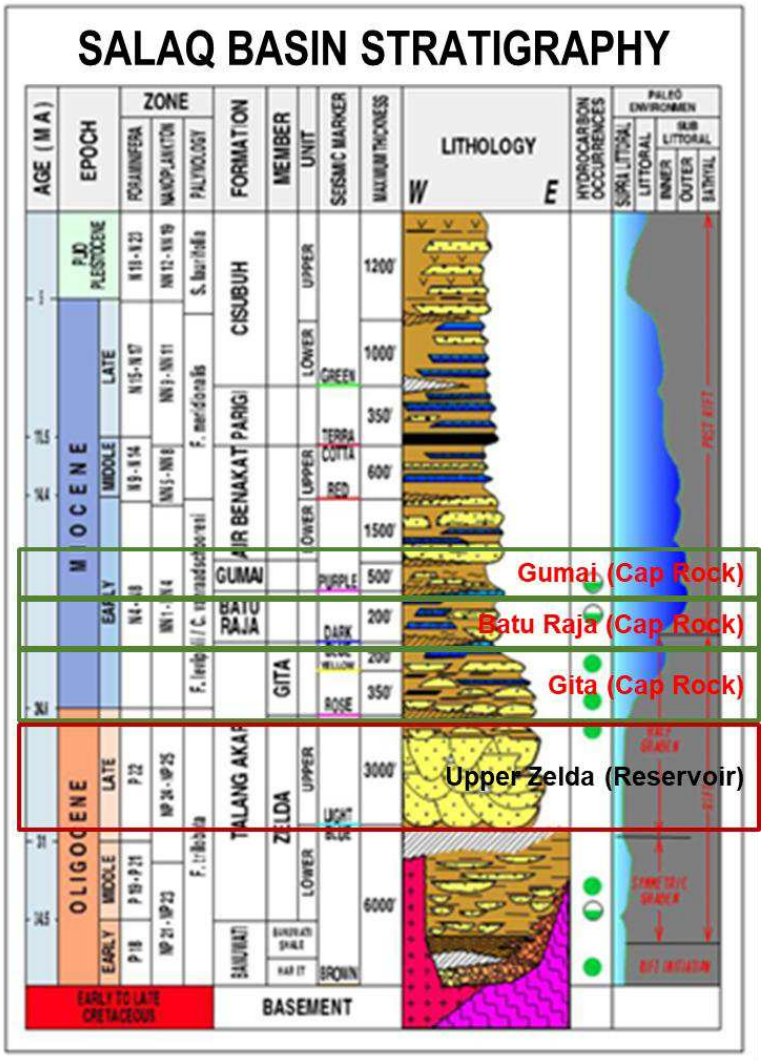


Figure 2. The general stratigraphy of the Salaq Basin (Ralanarko et al, 2020)

3. LITERATURE REVIEW

Caprock integrity assessment for CCS commonly integrates elastic properties, strength parameters, and failure criteria (Zoback, 2010; Rutqvist, 2012). Shale caprocks typically exhibit pressure-dependent strength behavior, with increasing confining pressure significantly enhancing compressive strength and shear resistance (Jaeger et al., 2007).

Young's modulus and Poisson's ratio are critical for evaluating stress redistribution and fracture initiation around injection wells (Warpinski & Teufel, 1987). Low Poisson's ratio and moderate Young's modulus generally favor mechanical stability under injection-induced stress changes.

Mohr–Coulomb parameters, particularly cohesion and friction angle, are widely used to evaluate shear failure risk and fault reactivation in CCS sites (Rutqvist et al., 2007). Laboratory-derived parameters provide conservative estimates for geomechanical modeling and injection pressure limits.

4. RESEARCH METHOD

4.1 Core Sampling and Preparation

Fifteen shale core plugs were prepared from six parent cores of Well SA-001, covering depths from 3546 to 3744 ft MD (**Table 1**). Samples were drilled to a diameter of approximately 25.2 mm and lengths between 52.1 and 54.7 mm, yielding L/D ratios of 2.07 – 2.18, compliant with ASTM D7012. Prior to testing, samples underwent CT-scan screening, solvent cleaning (toluene and methanol), and oven drying to remove residual fluids.

4.2 Rock Mechanics Testing

Uniaxial Compressive Strength (UCS) and Triaxial Compressive Strength (TCS) tests were conducted under confining pressures of 0 – 9.32 MPa. Axial and radial strains were continuously recorded to generate stress–strain curves.

Table 1. Shale core plugs were prepared from six parent cores of Well SA-001, covering depths from 3546 to 3744 (Baturaja Formation to Gita Formation)

No.	Depth (ft MD)	Lithology	Visible Features	Core Condition	Remarks
1	3546	Shale (Baturaja Fm)	Minor natural fractures, intact surface	Good	Representative core used for UCS and triaxial tests
2	3562	Shale (Baturaja Fm)	Bedding planes visible, slight breakage	Fair	Weaker interval; consistent with low UCS and Young's modulus
3	3665	Shale (Gita Fm)	Massive texture, minimal fractures	Very good	Mechanically competent interval; high UCS and stiffness
4	3710	Shale (Gita Fm)	Intact core, no visible damage	Excellent	Strong caprock interval; highest cohesion observed
5	3744	Shale (Gita Fm)	Pre-existing fractures, partial disintegration	Poor	One specimen fractured prior to triaxial loading



Note:
Core condition classification is based on visual inspection prior to laboratory testing. Cores described as *poor* quality were treated conservatively in strength interpretation and Mohr–Coulomb fitting.

4.3 Elastic Modulus Determination

Static elastic parameters, including Young's modulus, Poisson's ratio, bulk modulus, and shear modulus were calculated from the linear elastic portion of the stress–strain curves using the average slope method.

4.4 Mohr–Coulomb Failure Analysis

The shear failure behaviour of the shale caprock was evaluated using the Mohr–Coulomb failure criterion, which is widely applied in rock mechanics and geomechanical studies of caprock integrity and fault reactivation (Jaeger et al., 2007; Zoback, 2010). In its classical form, the criterion is expressed as:

$$\tau_f = C + \sigma_n' \tan \varphi \quad (1)$$

where τ_f is the shear stress at failure; σ_n' is the effective normal stress acting on the failure plane; C is the cohesion; and φ is the internal friction angle.

For triaxial compression conditions, the Mohr–Coulomb criterion can be written in terms of the principal stresses at failure (Jaeger et al., 2007):

$$\sigma_1 = m\sigma_3 + b \quad (2)$$

with

$$m = \frac{1+\sin \varphi}{1-\sin \varphi}, b = \frac{2C\cos \varphi}{1-\sin \varphi} \quad (3)$$

The internal friction angle and cohesion were obtained from the slope and intercept of the linear regression between peak axial stress σ_1 and confining pressure σ_3:

$$\sin \varphi = \frac{m-1}{m+1}, C = b\frac{1-\sin \varphi}{2\cos \varphi} \quad (4)$$

The friction coefficient was calculated as:

$$\mu = \tan \varphi \quad (5)$$

For each test condition, the normal stress σ_n and shear stress τ acting on the failure plane were calculated assuming a Mohr–Coulomb failure plane orientation of $\theta = 45° + \varphi/2$, which is commonly adopted for brittle rock failure analysis (Jaeger et al., 2007; Zoback, 2010):

$$\sigma_n = \frac{\sigma_1+\sigma_3}{2} - \frac{\sigma_1-\sigma_3}{2}\sin \varphi \quad (6)$$

$$\tau = \frac{\sigma_1-\sigma_3}{2}\cos \varphi \quad (7)$$

These formulations ensure internal consistency between the measured triaxial compression strength data, Mohr circles, and the derived Mohr–Coulomb failure envelope, which is critical for reliable caprock integrity assessment in CCS studies (Rutqvist et al., 2007; Rutqvist, 2012).

5. RESULTS AND DISCUSSION

5.1 Triaxial Compressive Strength Behavior

Ultimate compressive strength values range from 10.23 to 112.46 MPa, increasing systematically with confining pressure (**Table 2** and **Figure 3**). This behavior reflects frictional strengthening and closure of microcracks under confinement, consistent with shale mechanical behavior reported in previous studies. Depth-dependent variability indicates heterogeneity within the shale interval, likely related to mineralogical composition and fabric.

Table 2. Triaxial compressive strength data of shale core samples from Well SA-001

No.	Depth (ft MD)	Confining Pressure (MPa)	Peak Axial Stress, σ_1 (MPa)
1	3546	0.00	22.25
2	3546	4.41	42.32
3	3546	8.83	56.66
4	3562	0.00	10.23
5	3562	4.43	14.15
6	3562	8.87	40.49
7	3665	0.00	40.33
8	3665	4.56	100.10
9	3665	9.12	94.82
10	3710	0.00	70.53
11	3710	4.63	101.76
12	3710	9.25	112.46
13	3744	0.00	10.67
14	3744	4.66	—*
15	3744	9.32	64.23

Note:
*) Sample fractured prior to loading and excluded from strength and Mohr–Coulomb analysis.

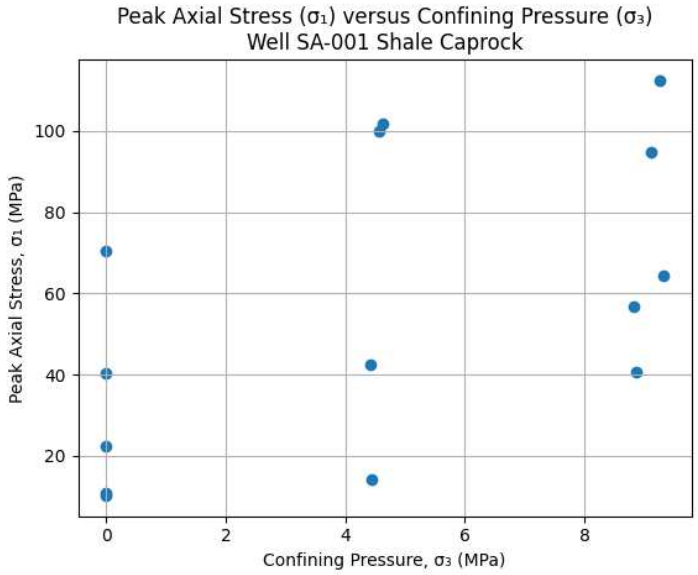


Figure 3. Peak axial stress (σ_1) as a function of confining pressure (σ_3) for shale core samples from Well SA-001. The increasing trend of σ_1 with σ_3 reflects pressure-dependent strengthening behavior typical of shale, forming the basis for Mohr–Coulomb failure

5.2 Elastic Properties

Young's modulus varies widely from 749,49 to 12,097 MPa (**Table 3**), indicating intervals of both ductile and stiff shale. Poisson's ratio values (0.12 – 0.20) suggest limited lateral strain, favorable for caprock stability under vertical stress changes (**Table 3**).
High bulk and shear moduli observed at depths around 3665 – 3710 ft indicate mechanically competent shale capable of resisting injection-induced deformation.

Table 3. Static elastic properties of shale core samples from Well SA-001

No.	Depth (ft MD)	Confining Pressure (MPa)	Poisson's Ratio, ν	Young's Modulus, E (MPa)	Bulk Modulus, K (MPa)	Shear Modulus, G (MPa)
1	3546	0.00	0.15	3161.90	1522.63	1370.09
2	3546	4.41	0.14	2846.00	1302.40	1252.86
3	3546	8.83	0.13	2910.70	1312.55	1287.46
4	3562	0.00	0.18	1105.00	578.05	467.67
5	3562	4.43	0.20	749.49	420.31	311.56
6	3562	8.87	0.16	1644.80	799.69	710.68
7	3665	0.00	0.12	11395.00	5046.95	5070.30
8	3665	4.56	0.13	12097.00	5415.44	5363.57
9	3665	9.12	0.14	9039.90	4195.63	3961.74
10	3710	0.00	0.12	9371.30	4066.35	4198.99
11	3710	4.63	0.16	8968.50	4333.86	3882.13
12	3710	9.25	0.14	9299.40	4267.35	4090.17
13	3744	0.00	0.16	1596.30	791.34	685.81
14	3744	9.32	0.13	4602.10	2080.33	2033.99

The combined variation of unconfined compressive strength (UCS), Young's modulus, and Poisson's ratio with depth (**Figure 4**) highlights pronounced mechanical heterogeneity within the shale caprock interval penetrated by Well SA-001. UCS values vary significantly across the studied depth range, with notably lower values at 3562 ft MD and 3744 ft MD, indicating mechanically weaker shale intervals that may control the onset of failure under stress perturbations. In contrast, higher UCS values at depths of 3665–3710 ft MD reflect stronger shale capable of sustaining higher stress levels.

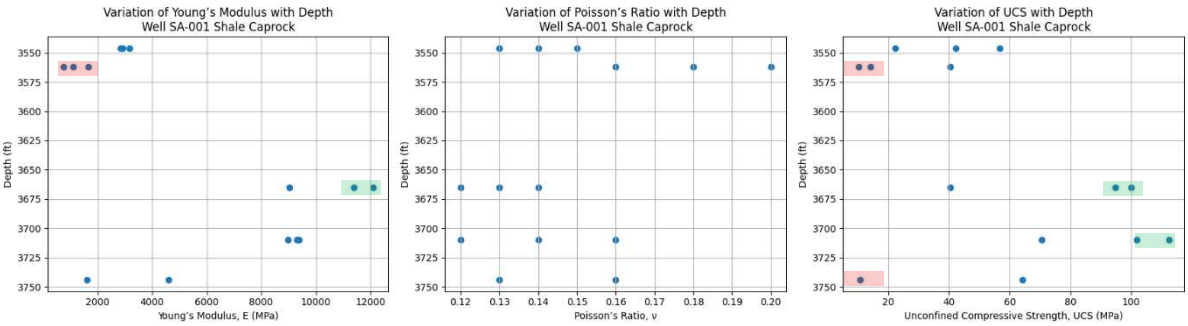


Figure 4. Depth-dependent variation of unconfined compressive strength (UCS), Young's modulus, and Poisson's ratio for shale core samples from Well SA-001, illustrating the mechanical heterogeneity and elastic–strength characteristics of the shale caprock.

Young's modulus exhibits a similarly heterogeneous pattern, ranging from less than 1 GPa to more than 12 GPa. Low Young's modulus values at 3562 ft MD suggest a more compliant and ductile shale, whereas the high modulus observed at depths of 3665–3710 ft MD indicates stiff and mechanically competent shale that is favorable for caprock performance by limiting deformation during CO_2 injection. Poisson's ratio values remain relatively low throughout the interval (0.12–0.20), implying limited lateral deformation and overall favorable elastic behavior for caprock integrity. Slightly higher Poisson's ratio values at the weaker intervals further emphasize the depth-dependent variability in elastic response.

Overall, the combined elastic and strength characteristics demonstrate that the shale caprock exhibits both mechanically weak and strong intervals, underscoring the importance of depth-specific geomechanical assessment. For CCS applications, these results indicate that injection pressure limits should be governed by the weakest shale intervals rather than averaged properties, to ensure long-term containment and minimize the risk of mechanical failure.

5.3 Mohr–Coulomb Parameters and Caprock Integrity

Mohr envelope analysis yields cohesion values of 1.76 – 17.36 MPa and friction angles between 33.14° to 45.50° (**Table 4**).

Table 4. Mohr–Coulomb strength parameters of shale caprock from Well SA-001

Depth (ft MD)	Cohesion, C (MPa)	Friction Angle, φ (°)	Friction Coefficient, μ
3546	5.88	36.27	0.73
3562	1.76	33.14	0.65
3665	10.47	45.50	1.02
3710	17.36	39.69	0.83
3744	2.23	44.71	0.99

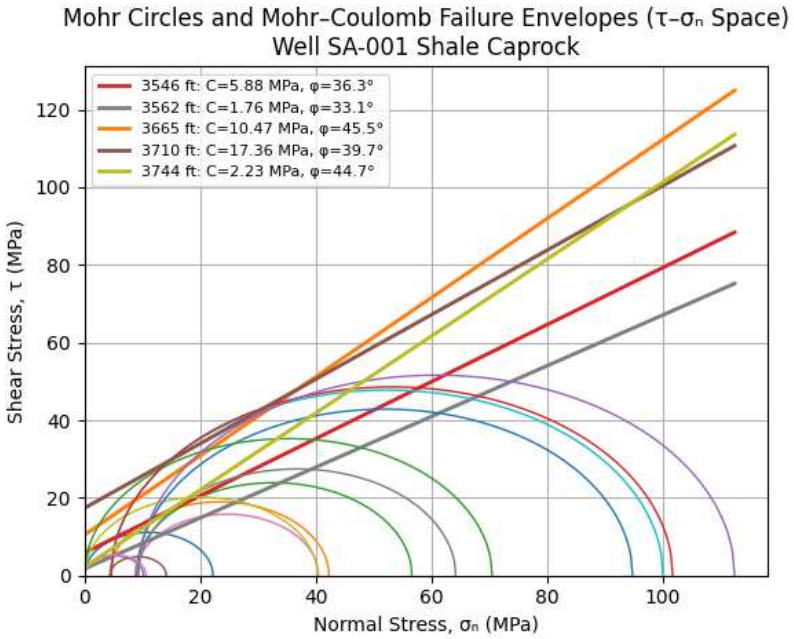


Figure 5. Mohr circles constructed from triaxial peak stresses (σ_1, σ_3) and the corresponding Mohr–Coulomb failure envelopes in τ–σ_n space for shale core samples from Well SA-001. Envelopes are fitted per depth interval to capture mechanical heterogeneity. The specimen at 3744 ft under $\sigma_3 \approx 4.66$ MPa that fractured prior to loading was *excluded from envelope fitting.*

These parameters indicate moderate to high shear strength, reducing the likelihood of shear failure or fault reactivation during CO_2 injection.

The tangency of the Mohr circles to the failure envelopes indicates that shear failure of the shale samples is well described by the Mohr–Coulomb criterion, confirming the validity of the derived cohesion and internal friction angle values. The systematic expansion of the Mohr

circles with increasing confining pressure reflects pressure-dependent strengthening behaviour, which is characteristic of shale and other frictional sedimentary rocks.

Clear depth-dependent variability in shear strength is observed. The shale interval at 3562 ft MD exhibits the lowest failure envelope, corresponding to low cohesion and friction angle, indicating a mechanically weaker zone that may control the onset of shear failure under injection-induced stress changes. In contrast, the envelopes for the 3665 ft and 3710 ft intervals are significantly steeper and higher, reflecting higher friction angles and cohesion values, and therefore greater resistance to shear failure. These intervals also coincide with higher elastic moduli, indicating mechanically competent and stiff shale.

At 3744 ft MD, the failure envelope shows relatively high frictional strength but low cohesion and is constrained by a limited number of valid triaxial data points due to premature specimen failure. This behaviour suggests the possible influence of weak planes, fabric anisotropy, or pre-existing microfractures, and therefore warrants conservative interpretation in caprock integrity assessment.

Overall, the Mohr circle analysis demonstrates that the shale caprock in Well SA-001 exhibits moderate to high shear strength, with mechanical heterogeneity across depth. For CCS applications, these results imply that injection pressure limits should be governed by the weakest shale intervals rather than average properties, and that depth-specific geomechanical modelling is essential to minimize the risk of shear failure or fault reactivation.

5.3.1 Mohr–Coulomb Parameters of Shale Caprock

Mohr–Coulomb failure envelopes were derived independently for each tested depth interval in Well SA-001 using triaxial compressive strength data (**Table 2**). This depth-specific approach is recommended for heterogeneous shale formations, where mechanical properties may vary significantly with mineralogy, fabric, and burial depth (Jaeger et al., 2007; Zoback, 2010).

The resulting internal friction angles range from 33.14° to 45.50°, while cohesion values vary between approximately 1.8 MPa to 17.4 MPa (**Table 4**). These values fall within the typical range reported for mechanically competent shale caprocks in sedimentary basins (Rutqvist et al., 2007; Rutqvist, 2012).

Shale samples at 3562 ft MD exhibit the lowest shear strength, characterized by a friction angle of approximately 33° and cohesion of about 1.8 MPa. This mechanical weakness is consistent with the relatively low unconfined compressive strength and low static Young's modulus observed at this depth (**Tables 2** and **Table 3**). Such intervals may act as mechanically controlling layers during CO_2 injection and should be considered conservative limits in injection pressure design (Zoback, 2010).

In contrast, shale intervals at 3665 ft MD to 3710 ft MD show significantly higher shear resistance. The 3665 ft interval is characterized by a high internal friction angle of approximately 45.5° and cohesion of about 10.5 MPa, accompanied by very high Young's modulus values (up to ~12 GPa). The 3710 ft interval exhibits the highest cohesion (~17.4 MPa) with a friction angle of approximately 39.7°, indicating a stiff and mechanically competent shale. Such properties are favorable for caprock performance under injection-induced stress perturbations (Rutqvist, 2012).

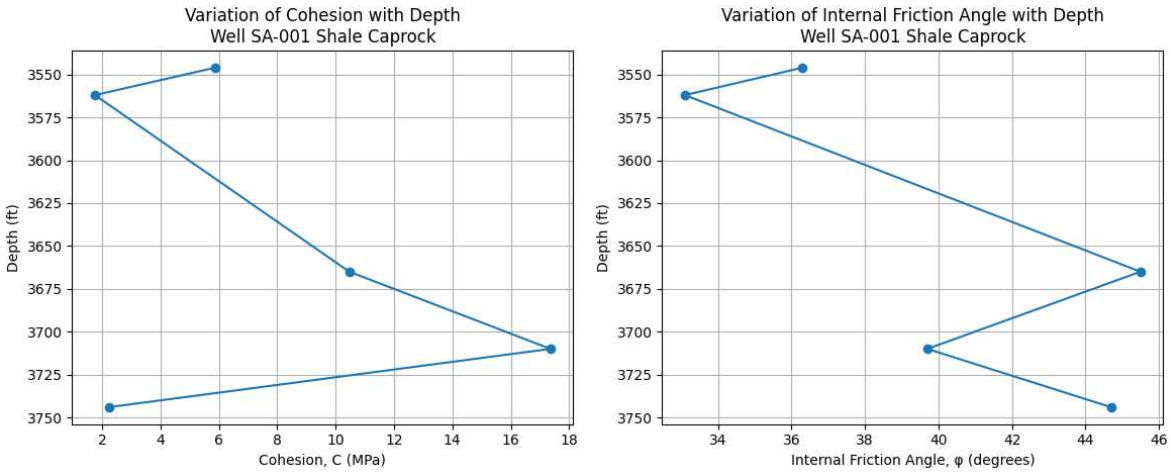


Figure 6. Variation of Mohr–Coulomb cohesion (C) with depth for shale core samples from Well SA-001. Significant depth-dependent variability is observed, with the lowest cohesion at 3562 ft MD and the highest cohesion at 3710 ft MD, indicating heterogeneous shear strength within the caprock interval. Variation of internal friction angle (φ) with depth for shale core samples from Well SA-001. Friction angles range from approximately 33° to 45°, indicating moderate to high frictional strength typical of shale caprocks, with notable depth-dependent variability.

At 3744 ft MD, although the friction angle remains high (~44.7°), the cohesion is relatively low (~2.2 MPa), and one specimen failed prior to triaxial loading. This behavior suggests the possible influence of weak planes, fabric anisotropy, or pre-existing microfractures, which are known to reduce effective caprock strength compared to intact rock estimates (Jaeger et al., 2007; Zoback, 2010).

5.3.2 Consistency with Mohr Circle Analysis

The calculated normal and shear stresses acting on the failure planes are fully consistent with the derived Mohr–Coulomb envelopes. For example, under unconfined conditions at 3546 ft MD ($\sigma_1 = 22.25$ MPa, $\sigma_3 = 0$ MPa), the computed stresses on the failure plane are approximately $\sigma_n = 4.5$ MPa and $\tau = 9.0$ MPa, which lie directly on the fitted failure envelope. Similar consistency is observed for all confining pressure levels and depth intervals, confirming the validity of the Mohr–Coulomb interpretation and its applicability to shale caprock assessment (Jaeger et al., 2007).

5.3.3 Implications for CCS Caprock Integrity

The derived Mohr–Coulomb parameters indicate that the shale caprock in Well SA-001 possesses moderate to high shear strength, particularly within the depth range of 3665–3710 ft MD, where both cohesion and friction angle are relatively high. Combined with low Poisson's ratios (0.12–0.16) and high elastic moduli, these properties suggest favorable mechanical behavior under CO_2 injection-induced stress changes (Warpinski & Teufel, 1987; Rutqvist, 2012).

5.4 Implications for CCS Development

The combination of moderate-to-high stiffness, low Poisson's ratio, and robust shear strength supports the suitability of the shale interval in Well SA-001 as an effective CCS caprock. Elastic heterogeneity, however, highlights the need for depth-specific geomechanical modeling.

6. CONCLUSION

This study presents a detailed geomechanical characterization of shale caprock in the Salaq Basin based on laboratory measurements of rock strength and elastic properties from Well SA-001. The results demonstrate that shale compressive strength increases significantly with confining pressure, reaching values of up to 112.46 MPa, indicating strong pressure-dependent mechanical behavior. Static elastic properties reveal mechanically competent shale intervals, with Young's modulus values up to 12,097 MPa and consistently low Poisson's ratios (0.12–0.20), which are favorable for caprock stability under injection-induced stress changes.

Mohr–Coulomb failure analysis indicates cohesion values ranging from approximately 2.2 to 17.4 MPa and internal friction angles between 33° and 45°, reflecting moderate to high shear strength of the shale caprock. Pronounced depth-dependent variability in both elastic and strength parameters highlights the presence of mechanically weaker intervals that may control the onset of shear failure during CO_2 injection. Consequently, injection pressure limits should be governed by the weakest shale intervals rather than averaged rock properties.

Overall, the integration of elastic properties and failure criteria provides a robust basis for assessing caprock integrity in CCS applications. While the shale interval penetrated by Well SA-001 is generally suitable as a sealing formation, reliable CCS development requires depth-specific geomechanical modeling that incorporates in-situ stress conditions and pore pressure effects to fully evaluate long-term containment and minimize the risk of mechanical failure.

AUTHOR CONTRIBUTIONS

Prof. Aris Buntoro, as the Lead researcher (Petroleum Engineer & Geoscientist – Universitas Pembangunan Nasional "Veteran" Yogyakarta) who summarized the research results for the writing of this paper; Allen Haryanto Lukmana (Geomechanics Specialist – Universitas Pembangunan Nasional "Veteran" Yogyakarta) as one of the researchers who made the geomechanical analysis in this study; Teddy Eka Putra (Geologist - Pertamina) and Dwandari Ralanarko (Subsurface Geoscience Lead - Pertamina) who have provided data and given permission for research and publication; all authors have approved the final version.

CONFLICT OF INTEREST

The authors declare no conflict of interest regarding the publication of this paper.

ACKNOWLEDGMENTS

The authors wish to thank Pusat Studi Migas & Panasbumi UPN "Veteran" Yogyakarta, Upstream Innovation – Pertamina Hulu Energy. This work was carried out with the support of Upstream Innovation – Pertamina Hulu Energy and PSP Migas & Panasbumi UPN "Veteran" Yogyakarta who has provided funding for this research, collaboration in geomechanical analysis for CCS study, data contributions and publication permits.

REFERENCES

[1.] ASTM D7012. (2014). *Standard Test Methods for Compressive Strength and Elastic Moduli of Intact Rock Core Specimens*. ASTM International.

[2.] Bradshaw, J., Bachu, S., Bonijoly, D., Burruss, R., Holloway, S., Christensen, N. P., & Mathiassen, O. M. (2007). CO_2 storage capacity estimation: Issues and development of standards. International Journal of Greenhouse Gas Control, 1(1), 62–68.
[3.] Doust, H., & Noble, R. A. (2008). Petroleum systems of Indonesia. Marine and Petroleum Geology, 25(2), 103–129.
[4.] Doust, H. (2016). Petroleum geology and potential for CCS in mature hydrocarbon basins of Southeast Asia. Energy Procedia, 86, 411–421.
[5.] Hall, R. (2002). Cenozoic geological and plate tectonic evolution of SE Asia and the SW Pacific, Journal of Asian Earth Sciences, 20(4), 353–431.
[6.] Jaeger, J. C., Cook, N. G. W., & Zimmerman, R. (2007). *Fundamentals of Rock Mechanics* (4th ed.). Blackwell Publishing.
[7.] Ralanarko et al (2020). Seismic Expression of Paleogene Talamngakar Formation – Salaq & Sunda Basins, Java Sea, Indonesia, Berita Sedimentologi, Number 48, November 2020, 21-74.
[8.] Rutqvist, J. (2012). The geomechanics of CO_2 storage in deep sedimentary formations. *Geotechnical and Geological Engineering*, 30, 525–551.
[9.] Rutqvist, J., Birkholzer, J., & Tsang, C. F. (2007). Coupled reservoir–geomechanical analysis of CO_2 injection. *International Journal of Greenhouse Gas Control*, 1(3), 299–315.
[10.] Siregar, M. S., Amin, T. C., & Sidarto. (1994). Stratigraphy and sedimentation of the Tertiary sequences in the Northwest Java Basin. Proceedings, Indonesian Petroleum Association (IPA), 23rd Annual Convention, 65–89.
[11.] Warpinski, N. R., & Teufel, L. W. (1987). Influence of geologic discontinuities on hydraulic fracture propagation. *Journal of Petroleum Technology*, 39(2), 209–220.
[12.] Zhu, H., Li, S., Wang, X., & Zhang, Y. (2018). Structural evolution and sedimentary infill of Cenozoic half-graben basins under extensional tectonics. Journal of Asian Earth Sciences, 156, 1–15.
[13.] Zoback, M. D. (2010). Reservoir Geomechanics. Cambridge University Press, Cambridge, UK.